

Pressure Difference Across the Free Surface of a Stable Convex Meniscus in a Possible $Ge_{1-x}Si_x$ Tube Growth by Edge-Defined Film-Fed Growth (EFG) Technique

Stefan Balint

Dept of Computer Science, West University of Timisoara
Blv: V. Parvan 4, 300223 Timisoara, Romania

Loredana Tanasie

Dept. of Computer Science, West University of Timisoara,
Blv: V. Parvan 4, 300223 Timisoara, Romania
tanasie@math.uvt.ro

Abstract

It is shown in this paper how to choose the pressure differences across the outer and inner free surfaces, in order to obtain a stable convex static meniscus with a prescribed size, in the case of a $Ge_{1-x}Si_x$ single crystal tube growth by EFG technique. The dependence of these pressure differences on the composition x is analyzed. The same tools as for a Ge or Si single tube growth are used. The results can be useful in a future experiment planning or manufacturing technology design.

Keywords: A1. Computer simulation, A2. Edge-defined film-fed growth, A2. Stepanov method, B2. Semiconducting silicon compounds

1 Introduction

The conventional melt growth techniques as Bridgman growth Ref[6-8] or Czochralski pulling rate Ref[1,4,5,9-18] of $Ge_{1-x}Si_x$ single-crystals typically produces ingots of circular or square cross-sections which need to be cut into hundreds of slices to produce wafers for: radiation detection, infrared optics, substrates for optoelectronics and microelectronics applications. Using these processes, it is difficult to produce thin wafers from an ingot without wasting

40-50% of material as kerf, during the cutting process. In addition, a subsequence of wafering is the surface damage, which needs to be removed by etching and polishing. The saving process followed by polishing increases the costs of the wafer production. The high costs of $Ge_{1-x}Si_x$ wafer affect their widespread use. For this reason the EFG technology can be more appropriate to produce $Ge_{1-x}Si_x$ single crystals with prescribed shapes and sizes, without any additional machining. For references concerning successful Si tube growth see Ref[3]. We have not found, in the literature, papers concerning $Ge_{1-x}Si_x$ tube growth by EFG technique, for $x \neq 0$ and $x \neq 1$. The fact that $Ge_{1-x}Si_x$ single crystal growth is possible by Czochralski technique for $x \neq 0$ and $x \neq 1$, suggests that the growth has to be possible also by EFG technique. It is shown in this paper how the pressure difference across the outer and inner free surfaces has to be chosen, in order to obtain a stable convex static meniscus with prescribed size and shape.

2 The free surfaces equations

In hydrostatic approximation, the equations of outer and inner free surface of the static meniscus for the growth of a single crystal tube by EFG technique are:

$$z_e'' = \frac{\rho \cdot g \cdot z_e - p_e}{\gamma} [1 + (z_e')^2]^{3/2} - \frac{1}{r} \cdot [1 + (z_e')^2] \cdot z_e', \quad r \in \left[\frac{R_{ge} + R_{gi}}{2}, R_{ge} \right], \quad (1)$$

and:

$$z_i'' = \frac{\rho \cdot g \cdot z_i - p_i}{\gamma} [1 + (z_i')^2]^{3/2} - \frac{1}{r} \cdot [1 + (z_i')^2] \cdot z_i', \quad r \in \left[R_{gi}, \frac{R_{ge} + R_{gi}}{2} \right], \quad (2)$$

respectively.

Here: γ is the surface tension, ρ is the melt density, g is the gravitational acceleration; z_e and z_i are the vertically upwards oriented coordinates with respect to the Oz axis, r is the radial coordinate with respect to Or axis, R_{ge} and R_{gi} are the outer and inner radii of the shaper, p_e and p_i are the pressure differences across the outer and inner free surface, respectively:

$$p_e = p_m - p_g^e - \rho \cdot g \cdot H \quad p_i = p_m - p_g^i - \rho \cdot g \cdot H \quad (3)$$

where: p_m denotes the hydrodynamic pressure in the meniscus melt; p_g^e and p_g^i are the gas pressures in the exterior and interior of the tube, respectively; H denotes the melt column height between the horizontal crucible melt level and the shaper top level (Fig 1.).

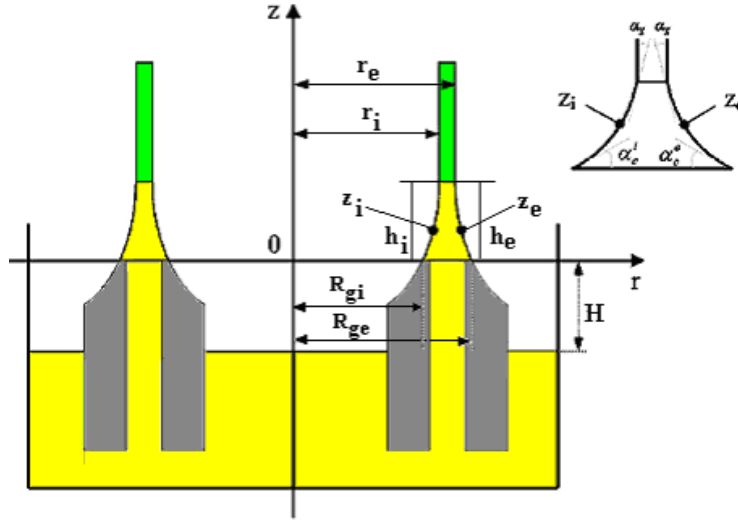


Figure 1: Prototype tubular crystal growth by EFG technique

The solution $z_e = z_e(r)$ of the equation (1) has to satisfy the following conditions:

$$\begin{cases} z'_e(r_e) = -\tan\left(\frac{\pi}{2} - \alpha_g\right) \\ z'_e(R_{ge}) = -\tan \alpha_c \\ z_e(R_{ge}) = 0 \text{ and } z_e(r) \text{ is strictly decreasing on } [r_e, R_{ge}] \end{cases} \quad (4)$$

where: $r_e \in \left[\frac{R_{gi} + R_{ge}}{2}, R_{ge}\right)$ is the tube outer radius; α_g is the growth angle; α_c is the contact angle between the outer free surface and the outer edge of the shaper top, $\alpha_c \in \left(0, \frac{\pi}{2} - \alpha_g\right)$ (Fig 1.).

The solution $z_i = z_i(r)$ of the equation (2) has to satisfy the following conditions:

$$\left\{ \begin{array}{l} z'_i(r_i) = \tan\left(\frac{\pi}{2} - \alpha_g\right) \\ z'_i(R_{gi}) = \tan \alpha_c \\ z_i(R_{gi}) = 0 \text{ and } z_i(r) \text{ is strictly increasing on } [R_{gi}, r_i] \end{array} \right. \tag{5}$$

where: $r_i \in \left(R_{gi}, \frac{R_{gi} + R_{ge}}{2} \right]$ is the tube inner radius; α_g is the growth angle; α_c is the contact angle between the inner free surface and the inner edge of the shaper top, $\alpha_c \in \left(0, \frac{\pi}{2} - \alpha_g \right)$ (Fig 1.).

In Ref [2] the following statements were shown:

Statement 2.1 *If there exists a solution $z_e(r)$ of the equation (1) which satisfies (4) and $z''_e(r) > 0$ then, for $n = \frac{R_{ge}}{r_e} \in \left(1, \frac{2R_{ge}}{R_{gi} + R_{ge}} \right]$ and p_e , the following inequalities hold:*

$$\begin{aligned} -\frac{n}{n-1} \cdot \gamma \cdot \frac{\frac{\pi}{2} - (\alpha_c + \alpha_g)}{R_{ge}} \cdot \cos \alpha_c + \frac{\gamma}{R_{ge}} \cdot \sin \alpha_c \leq p_e \leq -\frac{n}{n-1} \cdot \gamma \cdot \\ \cdot \frac{\frac{\pi}{2} - (\alpha_c + \alpha_g)}{R_{ge}} \cdot \sin \alpha_g + \frac{n-1}{n} \cdot \rho \cdot g \cdot R_{ge} \cdot \tan\left(\frac{\pi}{2} - \alpha_g\right) + n \cdot \frac{\gamma}{R_{ge}} \cdot \cos \alpha_g \end{aligned} \tag{6}$$

Consequence. If for $r_e = \frac{R_{gi} + R_{ge}}{2}$, eq (1) has a solution $z_e(r)$ which satisfies (4) and $z''_e(r) > 0$, then the following inequalities hold:

$$\begin{aligned} -2 \cdot \gamma \cdot \frac{\frac{\pi}{2} - (\alpha_c + \alpha_g)}{R_{ge} - R_{gi}} \cdot \cos \alpha_c + \frac{\gamma}{R_{ge}} \cdot \sin \alpha_c \leq p_e \leq -2 \cdot \gamma \cdot \\ \cdot \frac{\frac{\pi}{2} - (\alpha_c + \alpha_g)}{R_{ge} - R_{gi}} \cdot \sin \alpha_g + \rho \cdot g \cdot \frac{R_{ge} - R_{gi}}{2} \cdot \tan\left(\frac{\pi}{2} - \alpha_g\right) + \frac{2 \cdot \gamma}{R_{gi} + R_{ge}} \cdot \cos \alpha_g \end{aligned} \tag{7}$$

Statement 2.2 *If for p_e (defined by (3)) and $n \in \left(1, \frac{2 \cdot R_{ge}}{R_{gi} + R_{ge}} \right)$ the following inequality holds:*

$$p_e < -\gamma \cdot \frac{n}{n-1} \cdot \frac{\frac{\pi}{2} - (\alpha_c + \alpha_g)}{R_{ge}} \cdot \cos \alpha_c + \frac{\gamma}{R_{ge}} \cdot \sin \alpha_c, \tag{8}$$

then there exists r_e in the closed interval $\left[\frac{R_{ge}}{n}, R_{ge}\right]$ and a solution $z_e(r)$ of the equation (1) which satisfies (4) and $z_e''(r) > 0$.

Statement 2.3 If for $1 < n' < n < \frac{2 \cdot R_{ge}}{R_{gi} + R_{ge}}$ and the outer pressure difference p_e the following inequalities hold:

$$-\gamma \cdot \frac{\frac{\pi}{2} - (\alpha_c + \alpha_g)}{R_{ge}} \cdot \frac{n'}{n' - 1} \cdot \sin \alpha_g + \rho \cdot g \cdot R_{ge} \cdot \frac{n' - 1}{n'} \cdot \tan \left(\frac{\pi}{2} - \alpha_g\right) + \frac{\gamma}{R_{ge}} \cdot n' \cdot \cos \alpha_g < p_e < -\gamma \cdot \frac{\frac{\pi}{2} - (\alpha_c + \alpha_g)}{R_{ge}} \cdot \frac{n}{n - 1} + \frac{\gamma}{R_{ge}} \cdot n \cdot \sin \alpha_c, \tag{9}$$

then there exists $r_e \in \left[\frac{R_{ge}}{n}, \frac{R_{ge}}{n'}\right]$ and a solution $z_e = z_e(r)$ of the equation (1) which satisfies (4) on $[r_e, R_{ge}]$ and $z_e''(r) > 0$.

Statement 2.4 If for $n \in \left(1, \frac{2 \cdot R_{ge}}{R_{gi} + R_{ge}}\right)$ and p_e the following inequality holds:

$$p_e > \frac{n - 1}{n} \cdot \rho \cdot g \cdot R_{ge} \cdot \tan \alpha_c + n \cdot \frac{\gamma}{R_{ge}}, \tag{10}$$

then there is no $r_e \in \left[\frac{R_{ge}}{n}, R_{ge}\right]$ such that the equation (1) has a solution which satisfies (4).

Comments. 1) The value of $p_e = p_m - p_g^e - \rho \cdot g \cdot H$ can be controlled by the values p_g^e and H . It is commonly accepted that $p_m = 0$.

2) The above statements offer the possibility to control the shape and the size of the outer free surface by the values of p_e . In the next section, it will be shown how this can be done in the case of a $Ge_{1-x}Si_x$ meniscus.

Statement 2.5 If there exists a solution $z_i(r)$ of the equation (2), which satisfies (5) and $z_i''(r) > 0$, then for $m = \frac{r_i}{R_{gi}} \in \left(1, \frac{R_{gi} + R_{ge}}{2 \cdot R_{gi}}\right]$ and p_i the following inequalities hold:

$$-\frac{1}{m - 1} \cdot \gamma \cdot \frac{\frac{\pi}{2} - (\alpha_c + \alpha_g)}{R_{gi}} \cdot \cos \alpha_c - \frac{\gamma}{R_{gi}} \cdot \cos \alpha_g \leq p_i \leq -\gamma \cdot \frac{1}{m - 1} \cdot \frac{\frac{\pi}{2} - (\alpha_c + \alpha_g)}{R_{gi}} \cdot \sin \alpha_g + (m - 1) \cdot \rho \cdot g \cdot R_{gi} \cdot \tan \left(\frac{\pi}{2} - \alpha_g\right) + \frac{1}{m} \cdot \frac{\gamma}{R_{gi}} \cdot \sin \alpha_c. \tag{11}$$

Consequence. If for $r_i = \frac{R_{gi} + R_{ge}}{2}$, eq (2) has a solution $z_i(r)$ which satisfies (5) and $z_i''(r) > 0$, then the following inequalities hold:

$$\begin{aligned} -2 \cdot \gamma \cdot \frac{\frac{\pi}{2} - (\alpha_c + \alpha_g)}{R_{ge} - R_{gi}} \cdot \cos \alpha_c - \frac{\gamma}{R_{gi}} \cdot \cos \alpha_g \leq p_i \leq -2 \cdot \gamma \cdot \frac{\frac{\pi}{2} - (\alpha_c + \alpha_g)}{R_{ge} - R_{gi}} \\ \cdot \sin \alpha_g + \rho \cdot g \cdot \frac{R_{ge} - R_{gi}}{2} \cdot \tan \left(\frac{\pi}{2} - \alpha_g \right) - \frac{2 \cdot \gamma}{R_{gi} + R_{ge}} \cdot \sin \alpha_c \end{aligned} \quad (12)$$

Statement 2.6 If for $m \in \left(1, \frac{R_{gi} + R_{ge}}{2 \cdot R_{gi}} \right)$ and p_i the following inequality holds:

$$p_i < -\gamma \cdot \frac{1}{m-1} \cdot \frac{\frac{\pi}{2} - (\alpha_c + \alpha_g)}{R_{gi}} \cdot \cos \alpha_c - \frac{\gamma}{R_{gi}} \cdot \sin \alpha_g, \quad (13)$$

then there exists r_i in the closed interval $[R_{gi}, m \cdot R_{gi}]$ and a solution $z_i(r)$ of the equation (2) which satisfies (5) and $z_i''(r) > 0$.

Statement 2.7 If for $1 < m' < m < \frac{R_{gi} + R_{ge}}{2 \cdot R_{gi}}$ and the inner pressure difference p_i the following inequalities hold:

$$\begin{aligned} -\frac{1}{m'-1} \cdot \gamma \cdot \frac{\frac{\pi}{2} - (\alpha_c + \alpha_g)}{R_{gi}} \cdot \sin \alpha_g + \rho \cdot g \cdot R_{gi} \cdot (m' - 1) \cdot \tan \left(\frac{\pi}{2} - \alpha_g \right) - \\ \frac{1}{m'} \cdot \frac{\gamma}{R_{gi}} \cdot \sin \alpha_g < p_i < -\gamma \cdot \frac{1}{m-1} \cdot \frac{\frac{\pi}{2} - (\alpha_c + \alpha_g)}{R_{gi}} \cdot \cos \alpha_c - \frac{\gamma}{R_{gi}} \cdot \cos \alpha_g, \end{aligned} \quad (14)$$

then there exists $r_e \in [m' \cdot R_{gi}, m \cdot R_{gi}]$ and a solution $z_i(r)$ of the equation (2) which satisfies (5) and $z_i''(r) > 0$.

Statement 2.8 If for $m \in \left(1, \frac{R_{gi} + R_{ge}}{R_{gi}} \right)$ and p_i the following inequality holds:

$$p_i > (m-1) \cdot \rho \cdot g \cdot R_{gi} \cdot \tan \alpha_c + \frac{\gamma}{R_{gi}}, \quad (15)$$

then there is no $r_i \in [R_{gi}, m \cdot R_{gi}]$ such that the equation (2) has a solution which satisfies (5).

Comments: . 1) The value of $p_i = p_m - p_g^i - \rho \cdot g \cdot H$ can be controlled by the values p_g^i and H. (It is commonly accepted that $p_m = 0$.)

2) The above statements offer the possibility to control the shape and the size of the inner free surface by the values of p_i . In the next section, it will be shown how to this can be done in the case of a $Ge_{1-x}Si_x$ meniscus.

3 The pressure differences for a stable convex static $Ge_{1-x}Si_x$ meniscus with a prescribed size

It will be shown in this section how the explicit formulas established theoretically, can be used for the choice of p_e and p_i in order to obtain a stable convex static $Ge_{1-x}Si_x$ meniscus with a prescribed size.

The computation for Ge 0.98 Si 0.02 tube when $R_{gi} = 0.0042[m]$ and $R_{ge} = 0.0048[m]$ are performed in MathCAD v.13.

The numerical values of $\rho, g, \gamma, \alpha_c, \alpha_g$ for Ge and Si are given in Table 1:

Table 1.

	Ge	Si
ρ	$5.6 \times 10^3 [kg/m^3]$	$2.5 \times 10^3 [kg/m^3]$
γ	$6.2 \times 10^{-1} [N/m]$	$7.2 \times 10^{-1} [N/m]$
α_g	$47^\circ = 0.82 [rad]$	$30^\circ = 0.523 [rad]$
α_c	$12^\circ = 0.209 [rad]$	$11^\circ = 0.192 [rad]$
g	$9.81 [m/s^2]$	$9.81 [m/s^2]$

It is assumed that $\rho, g, \gamma, \alpha_c, \alpha_g$ for $Ge_{1-x}Si_x$ are given by the formulas [4]:

$$\begin{aligned}
 \rho(x) &= 5.6 \cdot 10^3 \cdot (1 - x) + 2.5 \cdot 10^3 \cdot x [kg/m^3] \\
 \gamma(x) &= 6.2 \cdot 10^{-1} \cdot (1 - x) + 7.2 \cdot 10^{-1} \cdot x [N/m] \\
 \alpha_c(x) &= 0.82 \cdot (1 - x) + 0.523 \cdot x [rad] \\
 \alpha_g(x) &= 0.209 \cdot (1 - x) + 0.192 \cdot x [rad]
 \end{aligned}
 \tag{16}$$

for $0 \leq x \leq 1$.

For the given numerical values ($x=0.02$), the pressure difference limits es-

tablished in Statement 1 and given by the inequality (6) are:

$$\begin{aligned}
 L_1^e(n) &= -\frac{n}{n-1} \cdot \gamma \cdot \frac{\frac{\pi}{2} - (\alpha_c + \alpha_g)}{R_{ge}} \cdot \cos \alpha_c + \frac{\gamma}{R_{ge}} \cdot \sin \alpha_c \\
 L_2^e(n) &= -\frac{n}{n-1} \cdot \gamma \cdot \frac{\frac{\pi}{2} - (\alpha_c + \alpha_g)}{R_{ge}} \cdot \sin \alpha_g + \frac{n-1}{n} \cdot \rho \cdot g \cdot R_{ge} \cdot \tan \left(\frac{\pi}{2} - \alpha_g \right) + \\
 &+ n \cdot \frac{\gamma}{R_{ge}} \cdot \cos \alpha_g.
 \end{aligned} \tag{17}$$

For different values of $n = \frac{R_{ge}}{r_e} \in \left(1, \frac{2R_{ge}}{R_{gi} + R_{ge}} \right]$, these limits are represented in Fig. 2:

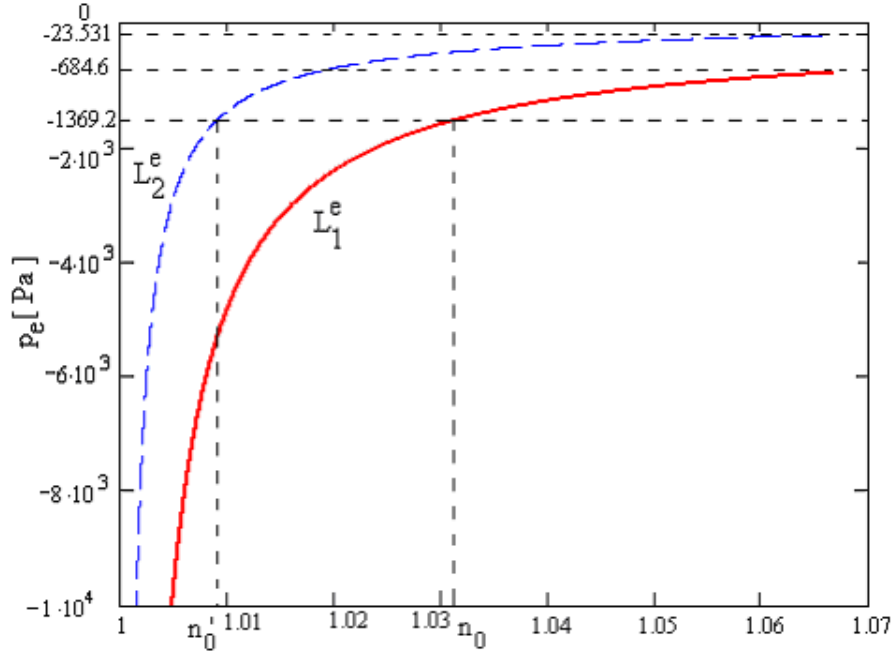


Figure 2: The pressure limits L_1^e and L_2^e for different values of n

The values of $L_1^e(n)$, $L_2^e(n)$ for $n = \frac{2 \cdot R_{ge}}{R_{gi} + R_{ge}}$ are:

$$L_1^e = -2 \cdot \gamma \cdot \frac{\frac{\pi}{2} - (\alpha_c + \alpha_g)}{R_{ge} - R_{gi}} \cdot \cos \alpha_c + \frac{\gamma}{R_{ge}} \cdot \sin \alpha_c = -684.6 \text{ [Pa]}$$

$$L_2^e = -2 \cdot \gamma \cdot \frac{\frac{\pi}{2} - (\alpha_c + \alpha_g)}{R_{ge} - R_{gi}} \cdot \sin \alpha_g + \rho \cdot g \cdot \frac{R_{ge} - R_{gi}}{2} \cdot \tan \left(\frac{\pi}{2} - \alpha_g \right) + \frac{2 \cdot \gamma}{R_{gi} + R_{ge}} \cdot \cos \alpha_g = -23.531 \text{ [Pa]}.$$

For a value p_e^0 of p_e , which is less than $L_1^e = -684.6$ [Pa] ($p_0 < L_1^e = -684.6$ [Pa]), there exists n_0 and n'_0 such that $p_e^0 = L_1^e(n_0) = L_2^e(n'_0)$ and $1 < n'_0 < n_0$. The numbers n_0 and n'_0 can be found solving the equations $L_1^e(n) = p_e^0$ and $L_2^e(n') = p_e^0$. For p_e^0 , n_0 , n'_0 the inequalities (9) hold. Hence, for every $p_e^0 < L_1^e = -684.6$ [Pa] the growth angle is reached at a point $r_e(p_e^0)$ which is in the range $\left[\frac{R_{ge}}{n_0}, \frac{R_{ge}}{n'_0} \right]$. For instance, if $p_e^0 = 2L_1^e = -1369.2$ [Pa] then $n_0 = 1.034407$, $n'_0 = 1.009851$ and the growth angle is reached at a point $r_e(p_e^0)$ in the range $[0.00464, 0.004753]$ [m].

Comments:

1. When $p_e < L_1^e = -684.6[\text{Pa}]$ decreases towards $-\infty$, then n_0 and n'_0 tend to 1, the range $\left[\frac{R_{ge}}{n_0}, \frac{R_{ge}}{n'_0}\right]$ becomes smaller and smaller thin and $r_e(p_e)$ tends to R_{ge} . Physically, this situation is not plausible because p_e is bounded below.
2. Neglecting for example p_m and p_g^e in the formula $p_e = p_m - p_g^e - \rho \cdot g \cdot H$, it is found that, for $p_e^0 = L_1^e = -684.6[\text{Pa}]$, the level difference H has to be $-\frac{L_1^e}{\rho \cdot g} = 1.26 \times 10^{-2}[\text{m}]$ and for $p_e^0 = 2 \cdot L_1^e = -1369.2[\text{Pa}]$, $H \approx -\frac{2 \cdot L_1^e}{\rho \cdot g} = 2.52 \times 10^{-2}[\text{m}]$.
3. For a value p_e^0 of p_e which is larger than $L_2^e = -23.531[\text{Pa}]$ there is no point r_e in the range $\left(\frac{R_{gi} + R_{ge}}{2}, R_{ge}\right)$ at which the growth angle is reached. This is a consequence of the Statement 2.1.
4. In fact, what happens when p_e is larger than $L_2^e = -23.531 [\text{Pa}]$ is not physically interesting because the point r_e , where the growth angle is eventually reached, is less than $\frac{R_{gi} + R_{ge}}{2}$.
5. What happens when p_e is in the range $[L_1^e, L_2^e] = [-686.4, -23.531][\text{Pa}]$ does not result from the above considerations. This can be clarified numerically integrating the equations:

$$\begin{cases} \frac{dz_e}{dr} = -\tan(\alpha_e) \\ \frac{d\alpha_e}{dr} = \frac{p_e - \rho \cdot g \cdot z_e}{\gamma} \cdot \frac{1}{\cos \alpha_e} - \frac{1}{r} \cdot \tan \alpha_e \end{cases} \quad (18)$$

for $z(R_{ge}) = 0$ and $\alpha(R_{ge}) = \alpha_c$.

1. In order to illustrate the above facts (also for $p_e < L_1^e$) we have solved (18) for $p_e \in [-4000, L_2^e][\text{Pa}]$. The values of $r_e(p_e)$, where the growth angle is reached and the corresponding meniscus height $h_e(p_e)$ for $p_e \in [-4000, -1000][\text{Pa}]$, are represented in Fig. 3 and Fig 4.

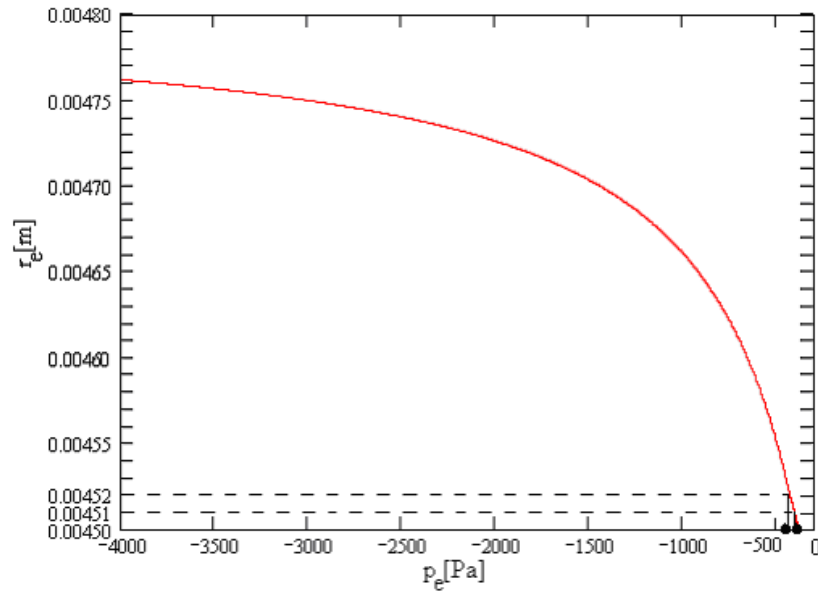


Figure 3: The dependence of the outer radius on the outer pressure difference

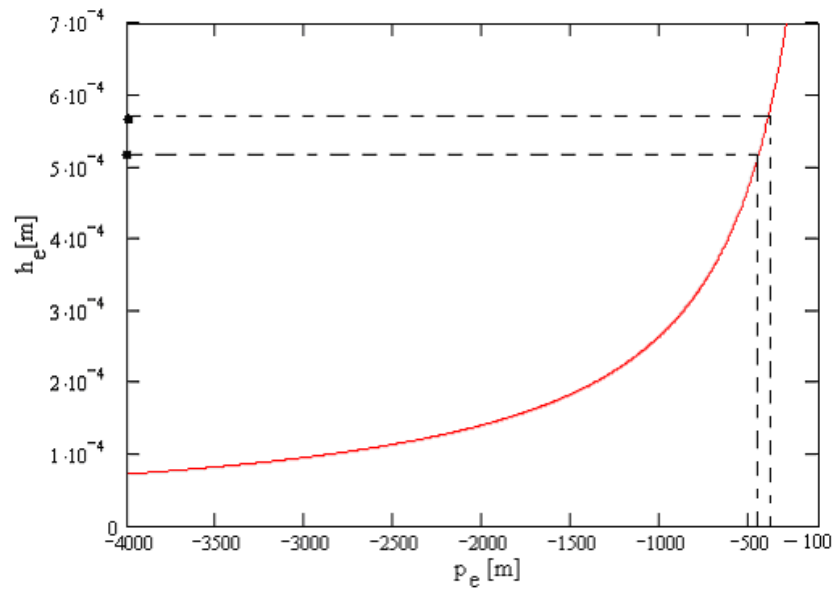


Figure 4: The dependence of the outer meniscus height on the outer pressure difference

Fig. 3 shows that, if p_e increases, $r_e(p_e)$ decreases and it will be physically interesting for $p_e < -300$ [Pa]. If p_e is higher than -300 [Pa], then $r_e(p_e)$ is less than $\frac{R_{gi} + R_{ge}}{2}$.

Moreover, it can be seen, for example, that tubes with the outer radius r_e in the range $[4.51 \times 10^{-3}, 4.52 \times 10^{-3}]$ [m], can be obtained when p_e is in the range $[-432.52, -412.81]$ [Pa] (Fig. 3).

The above presented results concern the outer free surface of the meniscus. For the inner free surface we have to consider the pressure limits established in Statement 2.5 and given by the inequalities (11):

$$L_1^i(m) = -\frac{1}{m-1} \cdot \gamma \cdot \frac{\frac{\pi}{2} - (\alpha_c + \alpha_g)}{R_{gi}} \cdot \cos \alpha_c - \frac{\gamma}{R_{gi}} \cdot \cos \alpha_g$$

$$L_2^i(m) = -\frac{1}{m-1} \cdot \gamma \cdot \frac{\frac{\pi}{2} - (\alpha_c + \alpha_g)}{R_{gi}} \cdot \sin \alpha_g + (m-1) \cdot \rho \cdot g \cdot R_{gi} \cdot \tan \left(\frac{\pi}{2} - \alpha_g \right) + \frac{1}{m} \cdot \frac{\gamma}{R_{gi}} \cdot \sin \alpha_c.$$

Fig. 5 shows these limits for different values of $m = \frac{r_i}{R_{gi}} \in \left(1, \frac{R_{gi} + R_{ge}}{2 \cdot R_{gi}} \right]$:

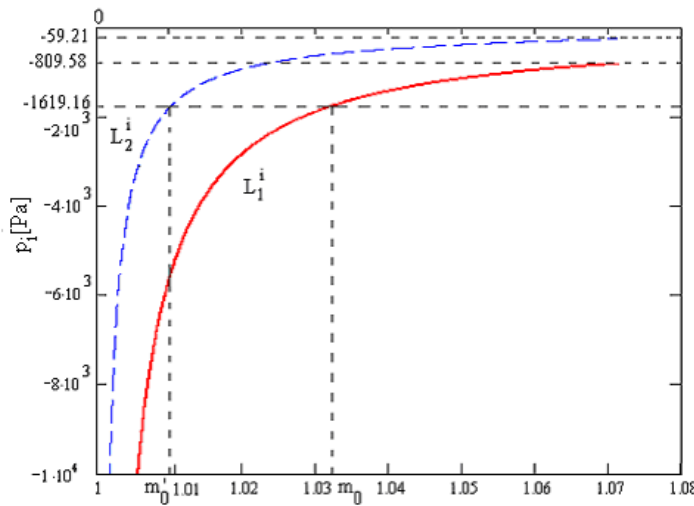


Figure 5: The pressure limits L_1^i and L_2^i for different values of m

The values of $L_1^i(m)$, $L_2^i(m)$ for $m = \frac{R_{gi} + R_{ge}}{2 \cdot R_{gi}}$ are:

$$L_1^i = -2 \cdot \gamma \cdot \frac{\frac{\pi}{2} - (\alpha_c + \alpha_g)}{R_{ge} - R_{gi}} \cdot \cos \alpha_c - \frac{\gamma}{R_{gi}} \cdot \cos \alpha_g = -809.58 [Pa]$$

$$L_2^i = -2 \cdot \gamma \cdot \frac{\frac{\pi}{2} - (\alpha_c + \alpha_g)}{R_{ge} - R_{gi}} \cdot \sin \alpha_g + \rho \cdot g \cdot \frac{R_{ge} - R_{gi}}{2} \cdot \tan \left(\frac{\pi}{2} - \alpha_g \right) + \frac{2 \cdot \gamma}{R_{gi} + R_{ge}} \cdot \sin \alpha_c = -59.215[\text{Pa}]$$

For a value p_i^0 of p_i , which is less than $L_1^i = -809.58[\text{Pa}]$ ($p_i^0 < L_1^i$), there exist m_0 and m'_0 such that $p_i^0 = L_1^i(m_0) = L_2^i(m'_0)$ and $1 < m'_0 < m_0$. The numbers m_0 and m'_0 can be found solving the equations $L_1^i(m) = p_i^0$ and $L_2^i(m') = p_i^0$. For p_i^0 , m_0 , m'_0 inequalities (14) hold. Hence, for every $p_i^0 < L_1^i = -809.58[\text{Pa}]$ the growth angle is reached at a point $r_i(p_i^0)$ which is in the range $[m'_0 \cdot R_{gi}, m_0 \cdot R_{gi}]$.

For instance, if $p_i^0 = 2 \cdot L_1^i = -1619.16[\text{Pa}]$ then $m_0 = 1.035023$, $m'_0 = 1.009769$ and the growth angle is reached at a point $r_i(p_i^0)$ in the range $[0.004241, 0.004347][\text{m}]$.

Comments:

1. When $p_i < L_1^i = -809.58[\text{Pa}]$ decreases towards $-\infty$, then m_0 and m'_0 tend to 1, the range $[m'_0 \cdot R_{gi}, m_0 \cdot R_{gi}]$ becomes smaller and smaller and $r_i(p_i)$ tends to R_{gi} . Physically, this situation is not plausible because p_i is bounded below.
2. Neglecting for example p_m and p_g^i in the formula of $p_i = p_m - p_g^i - \rho \cdot g \cdot H$, it is found that for $p_i^0 = L_1^i = -809.58[\text{Pa}]$ the level difference H has to be $H \approx -\frac{L_1^i}{\rho \cdot g} = 1.5 \times 10^{-2}[\text{m}]$ and for $p_i^0 = 2 \cdot L_1^i = -1619.16[\text{Pa}]$, it has to be $H \approx -\frac{2 \cdot L_1^i}{\rho \cdot g} = 3 \times 10^{-2}[\text{m}]$.
3. For a value p_i^0 of p_i which is greater than $L_2^i = -59.215[\text{Pa}]$, there is no point r_i in the range $\left(R_{gi}, \frac{R_{gi} + R_{ge}}{2} \right)$ at which the growth angle is reached. This is a consequence of the Statement 5.
4. In fact, what happens when p_i is larger than $L_2^i = -59.215 [\text{Pa}]$ is not so interesting from the physical point view because r_i , for which the growth angle eventually is reached, is larger than $\frac{R_{gi} + R_{ge}}{2}$.
5. What happens when p_i is in the range $[L_1^i, L_2^i] = [-809.56, -59.215][\text{Pa}]$ does not result from the above considerations. This can be clarified

integrating numerically the equations:

$$\begin{cases} \frac{dz_i}{dr} = \tan \alpha_i \\ \frac{d\alpha_i}{dr} = \frac{\rho \cdot g \cdot z_i - p_i}{\gamma} \cdot \frac{1}{\cos \alpha_i} - \frac{1}{r} \cdot \tan \alpha_i \end{cases} \quad (19)$$

for $z(R_{gi}) = 0$ and $\alpha(R_{gi}) = \alpha_c$.

In order to illustrate the above facts (also for $p_i < L_1^i$) we have solved (19) for $p_i \in [-4000, L_2^i][\text{Pa}]$. The values of $r_i(p_i)$, where the growth angle is reached, and the corresponding meniscus height $h_i(p_i)$, for $p_i \in [-4000, -100][\text{Pa}]$, are represented in Fig. 6 and Fig 7.:

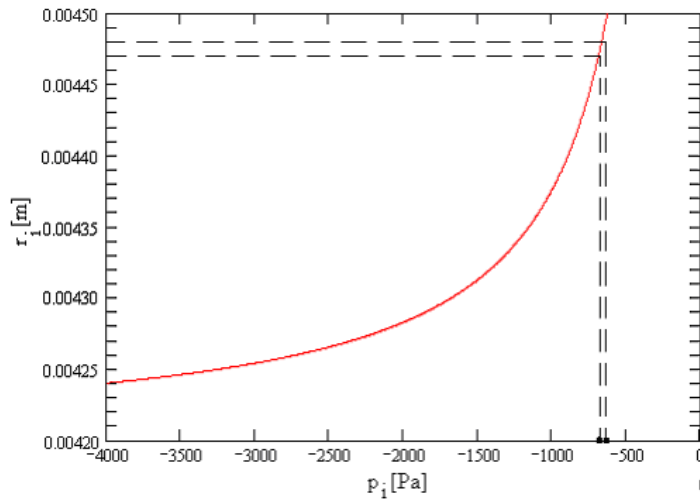


Figure 6: The dependence of the inner radius on the inner pressure difference

Fig. 6 shows that if p_i increases then $r_i(p_i)$ increases as well and it is physically interesting for $p_i < -600[\text{Pa}]$. If p_i is higher than $-600[\text{Pa}]$, then $r_i(p_i)$ is larger than $\frac{R_{gi} + R_{ge}}{2}$.

Moreover, it can be seen, for example, that tubes with inner radius r_i in the range $[4.48 \times 10^{-3}, 4.49 \times 10^{-3}][\text{m}]$ can be obtained when p_i is in the range $[-668.21, -648.43][\text{Pa}]$ (Fig. 6).

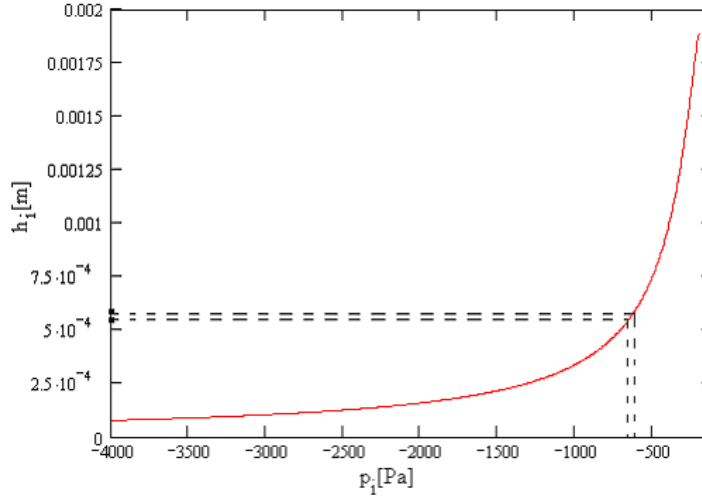


Figure 7: The dependence of the inner meniscus height on the inner pressure difference

Fig. 7 shows that if p_i increases then $h_i(p_i)$ increases too. When p_i is in the range $[-668.21, -648.43]$ [Pa] then $h_i(p_i)$ is in the range $[5.34 \cdot 10^{-4}, 5.53 \cdot 10^{-4}]$ [m].

All these results are dependent on x , which define the composition of the $Ge_{1-x}Si_x$ tube, and on the shaper radii R_{gi}, R_{ge} . For instance, in Section 4 the dependence on the composition x is analyzed for the fixed shaper radii $R_{gi} = 0.0042$ [m], $R_{ge} = 0.0048$ [m].

4 The dependence of the pressure difference on the $Ge_{1-x}Si_x$ tube composition x

The dependence of the limits:

$$L_1^e(x) = -2 \cdot \gamma \cdot \frac{\frac{\pi}{2} - (\alpha_c + \alpha_g)}{R_{ge} - R_{gi}} \cdot \cos \alpha_c + \frac{\gamma}{R_{ge}} \cdot \sin \alpha_c$$

$$L_2^e(x) = -2 \cdot \gamma \cdot \frac{\frac{\pi}{2} - (\alpha_c + \alpha_g)}{R_{ge} - R_{gi}} \cdot \sin \alpha_g + \rho \cdot g \cdot \frac{R_{ge} - R_{gi}}{2} \cdot \tan \left(\frac{\pi}{2} - \alpha_g \right) + \frac{2 \cdot \gamma}{R_{gi} + R_{ge}} \cdot \cos \alpha_g$$

$$L_1^i(x) = -2 \cdot \gamma \cdot \frac{\frac{\pi}{2} - (\alpha_c + \alpha_g)}{R_{ge} - R_{gi}} \cdot \cos \alpha_c - \frac{\gamma}{R_{gi}} \cdot \cos \alpha_g$$

$$L_2^e(x) = -2 \cdot \gamma \cdot \frac{\frac{\pi}{2} - (\alpha_c + \alpha_g)}{R_{ge} - R_{gi}} \cdot \sin \alpha_g + \rho \cdot g \cdot \frac{R_{ge} - R_{gi}}{2} \cdot \tan \left(\frac{\pi}{2} - \alpha_g \right) - \frac{2 \cdot \gamma}{R_{ge} + R_{gi}} \cdot \sin \alpha_c$$

on the composition x were found using the formulas (15).

These dependences are presented in Fig. 8. and Fig. 9:

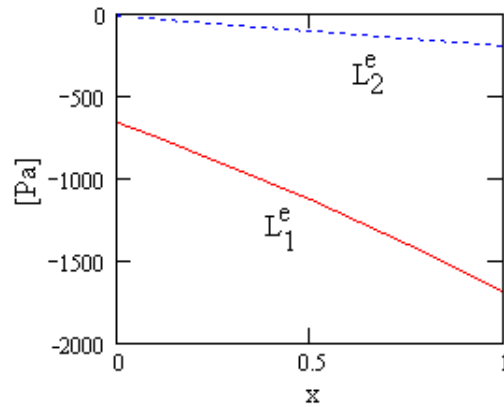


Figure 8: The dependence of the pressure limits L_1^e and L_2^e on the composition

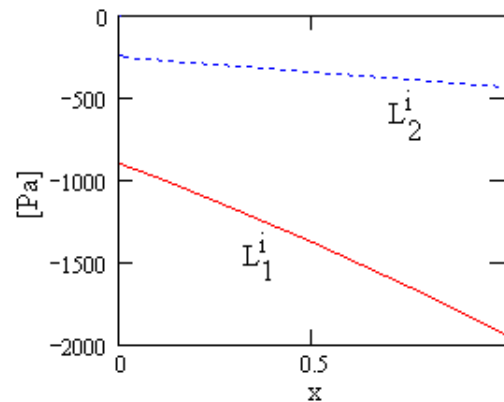


Figure 9: The dependence of the pressure limits L_1^i and L_2^i on the composition

Figs. 8, 9 show that when x increases, $L_1^e(x)$, $L_2^e(x)$, $L_1^i(x)$, $L_2^i(x)$ decrease and the differences $L_2^e(x) - L_1^e(x)$, $L_2^i(x) - L_1^i(x)$ increase.

The dependence of the estimated ranges $\left[\frac{R_{ge}}{n_0}, \frac{R_{ge}}{n_0'} \right]$, $[m_0' \cdot R_{gi}, m_0 \cdot R_{gi}]$ on the composition x for $p_e^0 = 2 \cdot L_1^e$ and $p_i^0 = 2 \cdot L_1^i$ respectively are represented in Fig. 10 and Fig. 11.

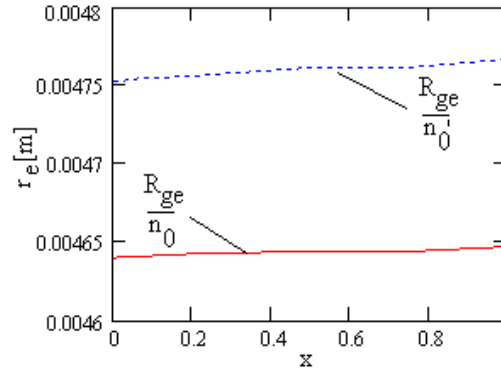


Figure 10: The dependence of the estimated ranges $\left[\frac{R_{ge}}{n_0}, \frac{R_{ge}}{n_0'}\right]$ on the composition

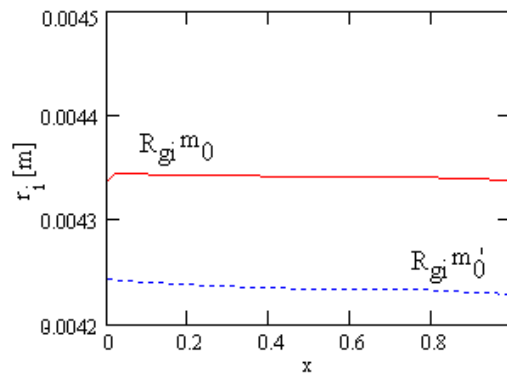


Figure 11: The dependence of the estimated ranges $[m_0' \cdot R_{gi}, m_0 \cdot R_{gi}]$ on the composition

Figs. 10, 11 show that the dependence of the estimated range of the outer and inner radius of the tube on the composition x is not significant.

The dependence of p_e on the composition x , used to obtain a $Ge_{1-x}Si_x$ tube of outer radius $r_e = 0.00455[m]$, is represented in Fig. 12.

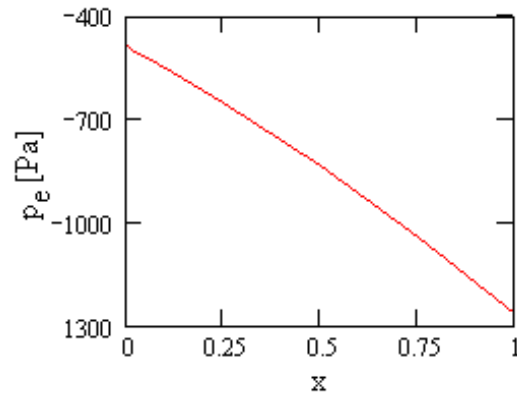


Figure 12: The dependence of the outer pressure p_e on the composition x

In Fig. 13. the corresponding meniscus heights are presented as function of the composition x .

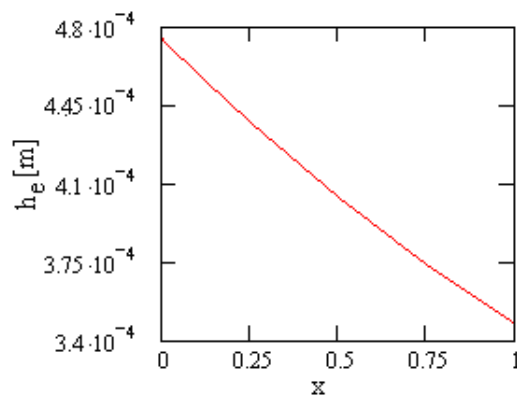


Figure 13: The dependence of the outer meniscus height h_e on the composition

The dependence of p_i on the composition x , used to obtain a $Ge_{1-x}Si_x$ tube of inner radius $r_i = 0.00445$ [m], is represented in Fig. 14.

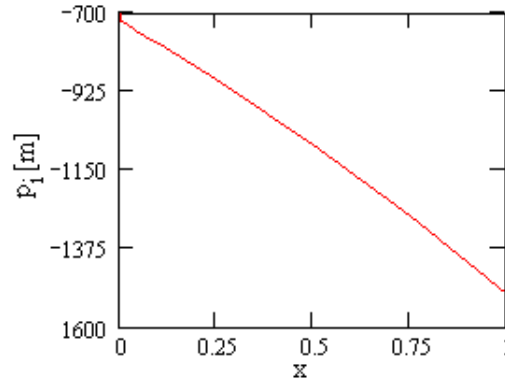


Figure 14: The dependence of the inner pressure p_i on the composition x

In Fig. 14. the corresponding meniscus height is presented as a function of the composition x .

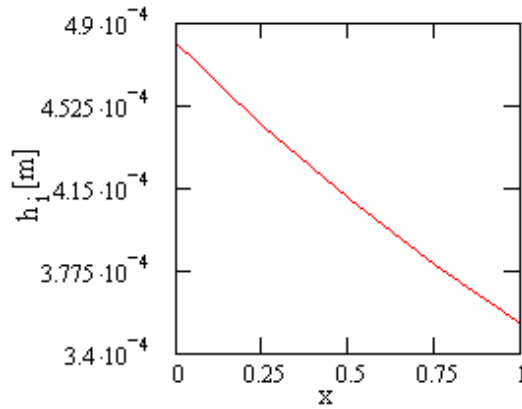


Figure 15: The dependence of the inner meniscus height h_i on the composition

In Fig. 16. the corresponding H , the melt column height between the horizontal crucible melt level and the shaper top level (in the condition $p_m = p_g^e$), is presented as a function of the composition x for the outer free surface.

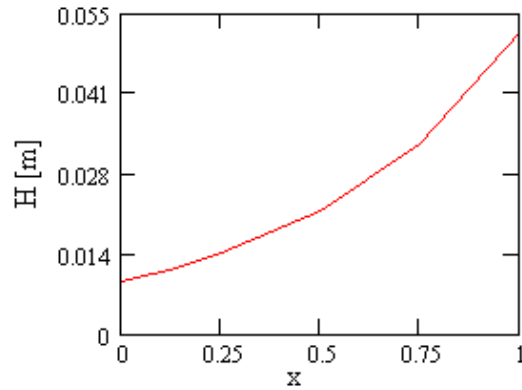


Figure 16: The dependence of the melt column height between the horizontal crucible melt level and the shaper top level on the composition x for the outer free surface

In Fig. 17. the corresponding H , the melt column height between the horizontal crucible melt level and the shaper top level (in the condition $p_m = p_g^i$), is presented as a function of the composition x for the inner free surface.

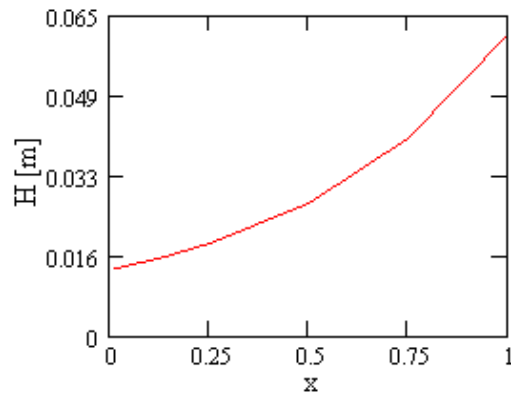


Figure 17: The dependence of the melt column height between the horizontal crucible melt level and the shaper top level on the composition x for the inner free surface

Conclusions

1. The pressure differences p_e , p_i across the outer and inner free surfaces needed for obtain a $Ge_{1-x}Si_x$ tube of given outer and inner radii, decrease when x increases.
2. The melt column height between the horizontal crucible melt level and the shaper top level, needed to obtain a $Ge_{1-x}Si_x$ tube of given outer and inner radii, has to be increased when x increases.

Acknowledgment

The authors thank to Romanian National Authority for Research for supporting this research under the grant no. 7/2007.

References

- [1] N. V. Abrosimov, S. N. Rossolenko, W. Thieme, A. Gerhardt, W. Schroder, *J. Crystal Growth*, **174** (1997) 182.
- [2] St. Balint, A.M. Balint, Inequalities for single crystal tube growth by edge-defined film-fed (EFG) technique submitted in 2007 to *Applied Mathematical Modelling*.
- [3] St. Balint, A.M. Balint, L. Tanasie, *J. Crystal Growth*, **310** (2008) 382.
- [4] Jiahe Chen, Deren Yang, Hong Li, Xiangyang Ma, Dualin Que, *J. Crystal Growth*, **291** (2006) 66.
- [5] B. Depuyt, A. Theuwis, I. Romandic, *Materials Science in Semiconductor Processing*, **9** (2006) 437.
- [6] Kenji Kadokura, Yukio Takano, *J. Crystal Growth*, **171** (1997) 56.
- [7] T.A. Lograsso, D.L. Schlagel, A.O. Pecharsky, *J. of Alloys and Compounds*, **363** (2005) 141.
- [8] C. Marin, A. Ostrogorsky, *J. Crystal Growth* **211** (2000) 378.
- [9] Xianhuan Niu, Weilian Zhang, Guoqi Lu, Zhongwei Jiang, *J. Crystal Growth*, **267** (2004) 424.
- [10] Xianhuan Niu, Weilian Zhang, Enhuai Zhang, Jungsheng Sun, *J. Crystal Growth*, **263** (2004) 167.
- [11] O. V. Smirnova, V.V. Kalaev, Yu. N. Makarov, N.V. Abrosimov, H. Riemann, V.N. Kurlov, *J. Crystal Growth* **303** (2007) 141.
- [12] Toshinori Taishi, Xinming Huang, Ichiro Yonega, Keigo Hoshikawa, *J. Crystal Growth*, **258** (2003) 58.
- [13] Deren Yang, jiahe Chen, Hong Li, Xiangyang Ma, Daxi Tian, Liben Li, Dualin Que, *J. Crystal Growth*, **292** (2006) 266.

- [14] Deren Yang, Xuegong Yu, Xiangyang Ma, Jin Xu, Liben Li, Duanlin Que, *J. Crystal Growth*, **243** (2002) 371.
- [15] I. Yonenaga, T. Taishi, X. Huang, K. Hoshikawa, *J. Crystal Growth*, **275** (2005) e501.
- [16] I. Yonenaga, M. Sakurai, M. Nonaka, T. Ayuzawa, M.H.F. Sluiter, Y. Kawazoe, *Physica B*, **340-342** (2003) 854.
- [17] I. Yonenaga and Y. Murakami, *J. Crystal Growth*, **191** (1998) 399.
- [18] I. Yonenaga, K. Sumino and A. Matsui, *J. Crystal Growth*, **183** (1998) 109.

Received: June, 2008